International Symposium of Research Students on Material Science and Engineering
December 20-22, 2004, Chennai, India
Department of Metallurgical and Materials Engineering, Indian Institute of Technology Madras

THE EFFECT OF COAL ASH COMPOSITION ON PROPERTIES OF WASTE-BASED GEOPOLYMERS

Louise M. Keyte, Grant C. Lukey and Jannie S.J. van Deventer
Department of Chemical and Biomolecular Engineering, The University of Melbourne, Victoria, AUSTRALIA

ABSTRACT

Geopolymers can be considered as low-temperature ceramic materials. These materials are formed by the alkali silicate dissolution of industrial wastes such as coal ash and blast furnace slag. At ambient conditions, the dissolved aluminium and silicon oxide species polymerise via a condensation reaction and re-precipitate to form the hardened geopolymer. Geopolymeric materials derived from aluminosilicate wastes such as coal ash can exhibit superior chemical and mechanical properties to ordinary Portland cement (OPC). The present work will investigate the relationship between coal ash composition and mechanical properties of various geopolymers. Analytical techniques including quantitative X-ray diffraction of devitrified coal fly ash enables the prediction of fly ash reactivity in a geopolymeric system. This can lead to optimisation and tailoring of geopolymer formulations to specific applications.

1. INTRODUCTION

Coal fly ash is often incorporated into Ordinary Portland Cement (OPC) as a value adding filler. In this system, coal fly ash is not highly reactive, but has been shown to improve properties such as workability and durability, and in some cases, up to 40% of the cement binder can be replaced with coal fly ash[1]. Research has since shown that coal fly ash can be alkali-activated, whereby dissolution of the glassy phases present in an alkaline medium results in the formation of a novel cementitious binder, referred to as a geopolymer. The potential for superior products to be formed using geopolymer technology, *viz*. improved strength, durability and acid resistance, has led to many researchers investigating ash from a wide variety of countries. From this work it has been established that most fly ashes could produce geopolymers with compressive strengths equal to and greater than that of OPC[2,3].

Geopolymerisation is a term that was first used by Davidovits[4] when it was discovered that various calcined clays, predominately calcined kaolinite (metakaolin), could be activated with alkaline solutions to produce hardened ceramic-like products at room temperature. Geopolymerisation now incorporates many types of aluminosilicate materials, including coal ash and industrial slag wastes. As coal ash is an industrial by-product, utilisation of such a material to create value-added products is of considerable commercial interest.

Coal ash is the waste by-product produced from the burning of pulverised coal in a coal-fired boiler. Coal deposits contain other minerals including kaolinite, pyrite and calcite in varying concentrations. These minerals do not combust as they pass through the coal burning flame, but the flame temperature is hot enough to melt them. As the melted minerals pass out through the flame, they are instantly cooled, and these particles are known as coal ash. This ash is generally separated into coarse and fine fractions, and it is the fine fraction that is known as coal fly ash.

Fly ash is a fine-grained, powder particulate material that is carried off in the flue gas and usually collected by means of electrostatic precipitators, bag houses, or mechanical collection devices such as cyclones.

At present there is only one commonly used classification system for coal combustion products, including fly ash, as defined by ASTM C 6 18. Pulverised coal fly ash is separated into two classes known as Class F and Class C[5]. The distinction between these two classes is based on the sum of the total silicon, aluminium and iron ($SiO_2 + Al_2O_3 + Fe_2O_3$) in the ash. When the sum is greater than 70%, an ash is classified as Class F. Class F fly ash generally originates from hard coal deposits (Anthracite and bituminous coal), whereas Class C fly ash originates from brown coal (lignite and sub bituminous coal). Fly ash can be further classified depending on iron content and alkali cation content. As most coal deposits contain some amount of pyrite or other iron mineral deposit, fly ash may contain up to as much as 20% iron oxide. Fly ash also generally demonstrates inter and intra-particle inhomogeneity, making it a very difficult material to analyse as every particle is compositionally very different and will respond differently to its environment.

Geopolymerisation reactions occur when an aluminium oxide and silicon oxide containing raw material is contacted with a highly alkaline solution. When using fly ash, the glass structure of the ash is rapidly attacked by hydroxide ions causing dissolution. At a pH > 8, glass dissolution occurs due to deprotonation by hydroxide ions[6] (Equation 1):

$$Si\text{-}OH + OH^- \rightarrow Si\text{-}O^- + H_2O \quad (1)$$

Water then attacks the glass via the following reaction (Equation 2):

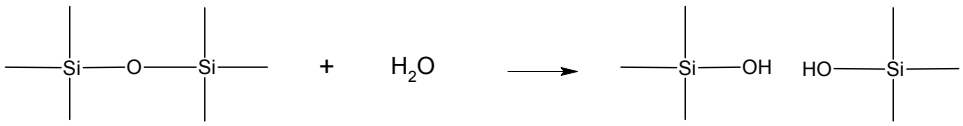

(2)

The new Si-OH bonds formed are consequently deprotonated, and the reaction continues. The rate at which glass dissolution occurs is largely dependent on the composition of the glass present in the fly ash. Vitreous silica type glass, highly substituted with alkali or alkaline earth metals, will react far more rapidly than glass with low amounts of these metals. This is because alkali and alkaline earth metals depolymerise vitreous silica networks, and consequently there are fewer bonds that have to be broken in order for dissolution to occur[7].

These mechanisms are different to those undertaken by coal fly ash when it is used in cement. The cement hydration reaction starts at a neutral pH and the water must diffuse into the cement. Protons exchange for cations, and hydroxide ions diffuse out in the initial stages of reaction. With time the cement hydration reactions generate hydroxide ions. This process is considerably slower than the mechanism described by Equations (1) and (2), as diffusion of the alkali must occur until the cement hydration reactions start. The fly ash glass dissolution is hence initially controlled by exchange of alkali ions in the glass with water[5].

A great deal of research into the physical and chemical structure of fly ash has been undertaken by various researchers in the 1980s[8-13]. However, this work was focused on relating fly ash structure to the behaviour of cement/fly ash blends. Since this time, geopolymer technology has emerged and very little research has been performed on how the physical and chemical structure of fly ash relates to the performance properties of geopolymer products formed. This paper will therefore investigate the physical and chemical properties of coal fly ash and correlate these properties to the coal fly ash behaviour in geopolymers.

2. EXPERIMENTAL METHODS

2.1 Materials

Fly ash A (Class F) and fly ash B (Class C) were obtained from power stations in New Zealand and Australia. Washed and classified sand (Cement Grade) was obtained from Unimin Australia. Sodium silicate solution (molar ratio SiO_2/Na_2O = 2.0, 29.4 wt% SiO_2) was obtained from PQ Australia. Laboratory grade reagents (NaOH, KOH) were obtained from Consolidated Chemicals, Australia. Distilled water was used throughout.

2.2 Characterisation

Compressive strength results were obtained conforming to ASTM C39 on an ELE compression machine using a loading rate of 0.9 kN/s. The cube sample dimension was 50 x 50 x 50mm for the mortars. All the values collected were the averages of three separate tests, with a standard deviation of less than 5%. Scanning electron microscopy (SEM) images were obtained using a Philips XL30 SEM. The fly ash samples were adhered to carbon tape and coated with gold. The fly ash samples were analysed by powder XRD analysis (Phillips PW 1800) using Cu Kα radiation, which was generated at 30mA and 40kV with an average wavelength of 1.54184 Å. The samples were step-scanned at 0.05^o 2θ and integrated at the rate of 2 s $step^{-1}$. Quantitative analysis was performed using Bruker-AXS Software: Diffrac*plus* Basic, Evaluation Package comprising the Diffrac*plus* Basic evaluation programs Eva, PDFMaint, DQuant, and some auxiliary programs. Optical light microscope images were obtained using an Olympus SZ 1145 using a Nikon Cool-Pix 990 digital camera. Devitrification of fly ash was performed by calcining samples at 900°C for 24 hours, with controlled cooling to minimise glass formation.

2.3 Synthesis

For compressive strength analysis, geopolymer samples were generated using a dry blend of 1 part coal fly ash to 2.1 parts dry, sieved sand and an activating solution of varying hydroxide and silicate concentration. All samples were cured at 23±0.5°C and greater than 95% humidity for 28 days.

3. RESULTS AND DISCUSSION

3.1 Physical Characterisation of Fly Ash

The morphology of fly ash has been studied extensively[14], and it is widely agreed that most fly ash particles are spherical and are of a particle size generally ranging from 1μm - 100μm. Some larger particles will be present however, and are generally irregular in shape, and may be a clump of spheres fused together. Most fly ash has a fairly large concentration of plerospheres, which are thin walled hollow spheres, with smaller included spheres. Cenospheres are also present in a lesser concentration, and these are simply hollow spheres.

Two fly ash samples were chosen for this investigation on the basis of two different coal sources. Fly ash A was generated from coal containing the minerals kaolinite, pyrite and quartz as well as small amounts of impurities including calcite. Fly ash B was generated from coal containing kaolinite, pyrite, quartz and calcite, as well as small amounts of impurities. Consequently, fly ash A is expected to be a Class F fly ash as the coal contains less than 10% calcite. Fly ash B is expected to be a Class C fly ash as the coal contains greater than 12% calcite. Table 1 outlines some of important physical properties of these fly ash samples.

Many researchers have published Scanning Electron Microscopy (SEM) images of fly ash particles at various resolutions; however, very little, if any, published work has shown images of

fly ash under an optical microscope. As shown by Figure 1, both fly ash A and fly ash B are heterogeneous (ie. contain different coloured particles). For example, the distribution of the iron oxide between different fly ash particles is not homogenous, as only about half of the particles are visibly black in fly ash A (Figure 1a), whereas a much smaller percentage are black in fly ash B (Figure 1b). Many particles are completely transparent or opaque white and contain no iron, whereas others are slightly pigmented with orange and brown colouring due to various impurities.

.The interparticle heterogeneity is more apparent when the coal fly ash is separated into particle size fractions (Figure 2a), and intraparticle heterogeneity is observable in larger particles, as shown in Figure 2b. These particles are of particular interest as they demonstrate the concept of phase separation in the glassy phases of fly ash, and this will be discussed in more detail later.

The colour of a fly ash particle reveals a great deal of information about its particular chemistry. For example, black particles will generally be unreactive as they will be either: (1) magnetite - a non-glassy component of fly ash; (2) an iron containing glass; (3) a glass with less reactivity than other types of vitreous silica; or (4) carbon - a non-glassy component of fly ash. It is the combination of these different colours that contribute to the overall appearance of a coal fly ash sample. From Table 1, fly ash A has a grey appearance, and it can be seen that this is due to the high concentration of black particles. Consequently, if it were possible to separate fly ash particles based on colour, then effective separation of particles into reasonably homogeneous fractions would be possible, as the colour of the particle is an indication of the chemical composition.

SEM images are also useful in demonstrating fly ash particle morphology, including the spherical nature of most fly ash particles (Figure 3a), plerospheres (Figures 3b and 3c), and the crystalline content of some particles (Figure 3d). Magnetic particles can also be detected when a particle with an irregular surface is located and the electron beam is moved closer during magnification (Figure 4a and b). The beam will repel these particles and they will shift position.

Although coal fly ash is an extremely complex material due to inter- and intraparticle heterogeneities, it is these very characteristics that allow physical observation of the compositional differences between particles. It can be expected from these observations that coal fly ash with a high concentration of black particles will be less reactive than a coal fly ash with a lower concentration, for example. Coal fly ash with larger particle size and lower concentrations of spheres can also be expected to be less reactive as small spherical particles generally have a high glassy composition, as glass formation is favoured for small particles as they quench more rapidly than larger particles[13]. Retention of spherical shape is also more likely due to rapid quenching, with no time available for the particle to collapse in on itself. Physical characterisation methods can further be used as relatively simple method of determining compositional changes in fly ash. If, for example, coal fly ash is classified in some manner to remove certain particles, such as iron, optical microscopy will reveal a change in the concentration of black particles. For these reasons, it is proposed that the behaviour of coal fly ash in a geopolymer system can be predicted based on physical observations of particle size, shape and colour. This aspect of the current work will be discussed in more detail when compressive strength results of the geopolymer binders studied are presented.

3.2 Chemical Characterisation of Fly Ash

As mentioned previously, fly ash displays interparticle and intraparticle heterogeneity, and this has been attributed to the process in which fly ash forms in a coal-fired power station. Coal is pulverised prior to burning, and consequently, as pulverised coal is not homogeneous, fly ash is the result of individual pieces of pulverised coal being melted and cooled rapidly, with insufficient time for these particles to come into contact with each other. Each fly ash particle is the residue from each individual piece of pulverised coal.

The minerals contained in the coal from which fly ash A and B are produced are mainly kaolinite, quartz, pyrite and calcite. When these minerals melt as the coal particles pass through the flame, a molten glass will form. As the rate of cooling is not controlled, some of the glass will cool quickly enough to remain vitreous, but some crystallisation will also occur. Table 2 outlines the transformations these minerals can undertake under these conditions[7].

It is important to note that all of these products can occur in any combination or concentration and in any fly ash particle, depending on the concentrations of the minerals in each piece of pulverised coal. For any given fly ash, using a combination of analytical techniques, the glassy phase concentration and the crystalline phase concentration, as well as the types and relative concentrations of these phases, can be determined. The glassy phase can be further analysed by devitrifying the fly ash. Heating the ash samples at high temperatures (>900^{o}C) for extended periods of time (>24h) will result in the glassy phase devitrifying into its corresponding crystal phase. From these results, the quantities and types of glassy phases in the fly ashes can be determined.

Table 3 shows the results of the two fly ash samples analysed using X-Ray Fluorescence (XRF) to determine the oxide composition of the main components. Quantitative X-Ray Diffraction (Q-XRD) was also performed to determine the relative concentrations of the amorphous glassy phases, the types of the crystalline phases present and their quantities.

The XRF results show that fly ash A is a Class F fly ash as it contains only 5.61% CaO, whereas fly ash B is classified as a Class C fly ash as it contains 19.11% CaO. It is interesting to note that both of the ashes contain around 1% TiO_2, which potentially acts as a nucleation site for crystal growth. Consequently, it is expected that some crystal formation will occur during cooling. Both of the ashes contain significant amounts of iron oxide, and it is expected that this will be present as magnetite and hematite (Figure 1), as well as being present in glassy phases. The Q-XRD results presented in Table 4 show that quartz and mullite (from kaolinite melt phase separation) are present, as well as magnetite, as is observed in Figure 4.

Comparing the results for fly ash A and B presented in Table 4, it is established that most of the calcium ions in fly ash B must be present in the glassy phase, while only in about half of the glassy phase of fly ash A. Fly ash A has a high concentration of magnetite, with almost half of the iron content being present as magnetite, as opposed to fly ash B which contains very little magnetite. Finally, the amorphous content of fly ash B is significantly greater than that of fly ash A, meaning that there is more material available to undergo geopolymerisation in fly ash B.

These results clearly indicate that the coal from which fly ash B is either much more homogeneous than that of fly ash A, or that the pulverisation mechanism leads to more homogeneous coal particles. This can be inferred from the lack of calcite and magnetite in this fly ash. If discrete coal particles contained only pyrite, or only calcite, then these phases would also be present in the fly ash, as glass phases cannot form from these minerals without the presence of a glass forming mineral such as kaolinite.

Finally, it can be seen that phase separation of kaolinite melt has occurred (ie. the presence of mullite in both fly ashes). Phase separation occurs in glass when the concentrations of the various elements is such that if rearrangement into two or more separate phases results in lower free energy, than the elements will exist as a homogeneous glass[6]. Consequently, glasses that contain aluminium and silicon may separate into a high alumina phase and a high silica phase to reduce free energy, which will result in the crystallisation of mullite. This then means that both fly ashes must contain vitreous silica phases, due to the presence of mullite. As mention previously, the lack of calcite in fly ash B reveals that most of the calcium ions must be present

in a glassy phase resulting in the possibility that calcium silicate and calcium aluminate type glasses may exist.

By confirming the presence of vitreous silica in the fly ash samples investigated in the current work, as well as calcium containing glass, demonstrates that the ash should be highly reactive in a geopolymer system. More specifically, the identification of the types of glass present and their concentrations will allow accurate prediction of the ions and molecules that will dissolve during geopolymerisation (ie. in a highly alkaline system), and this should allow accurate prediction of the setting time and strength of the geopolymers formed.

By devitrification of the fly ash samples, the types of glasses present can be identified from the crystal structures that form. This method should allow for determination of the glass phase reactivity. Devitrification is an established method for the determination of glassy phases in fly ash; however very little, if any, research has been performed on quantifying these phases to determine the quantity of phases present, and using this information to predict the properties of geopolymer products that will form. Table 5 presents the results from devitrification experiments performed on fly ash A and B in the current work.

Both fly Ash A and fly ash B contain similar amounts of vitreous silica, and the concentration of calcium ions can be estimated based on the crystalline phases formed. Formation of gehlenite, anorthite and wollastonite in the concentrations shown in Table 5 for fly ash B indicates that approximately half of the calcium ions are present in glasses of these compositions. Vitreous silica glasses will be highly reactive as calcium ions depolymerise silica glass networks, and consequently, dissolution will occur rapidly. However, if the vitreous silica glasses contain high concentrations of aluminium (gehlenite, anorthite and diopside), then they will be more stable and less reactive. These results show that the vitreous silica in fly ash B, accounts for approximately 54% of the ash, and it contains nearly half the calcium ions present in the fly ash. Fly ash A however contains no highly reactive glassy phases, and the vitreous silica will contain few calcium ions (Table 5).

From these results it is expected that fly ash B will be significantly more reactive than fly ash A in a geopolymer system. Furthermore, the compressive strength of geopolymer samples should be significantly higher when fly ash B is used compared to fly ash A, because more fly ash B will dissolve due to the depolymerisation of the vitreous silica network by calcium[6]. This is a very significant result because it allows for the analysis of other fly ashes. For example, if all of the calcium in a particular ash of similar oxide composition as fly ash B, is present in a gehlenite phase, then it could be predicted that both fly ash B and the new ash would probably react in a similar manner, thereby forming similar products with essentially the same physical properties. Moreover, these results clearly demonstrate that the prediction of fly ash behaviour during geopolymerisation can be achieved by analysing the phases that form from devitrification and comparing these phases to the original sample to estimate the quantities of glasses present in the original fly ash.

3.3 Properties of Geopolymers formed from Fly Ash

To understand the behaviour of fly ash during geopolymerisation, the compressive strength of geopolymer samples has been determined at different activator concentrations. It is important to note that geopolymers generated from fly ash B had a significantly faster setting time (<10 mins) than those from fly ash A (>1 day). This is expected because fly ash B contained a high proportion of calcium in glassy phases (Tables 4 and 5).

Some preliminary compressive strength results obtained in the current work are presented in Table 6. These results demonstrate that the initial compressive strength profiles of fly ash A

and B are similar; however materials generated from fly ash B had setting times of less than 10 minutes compared to setting times of greater than 1 day for fly ash A. Therefore, depending upon the glass composition of the specific fly ash, it is possible to achieve comparable strengths but with a significantly shorter initial setting time. This is an important consideration for successful commercial application of the technology.

As more of the fly ash will dissolve due to the depolymerisation of the vitreous silica network by calcium[6], the ultimate compressive strength of materials generated by fly ash B is expected to be significantly higher than those generated from fly ash A, especially at elevated curing temperatures. Although subject to on-going work, it has been observed that geopolymers generated using fly ash A had an ultimate compressive strength of 9.5MPa, whereas a geopolymer generated from fly ash B had an ultimate compressive strength of 47.5MPa.

4. CONCLUSIONS

Analytical techniques such as physical characterisation using microscopy and chemical characterisation using XRF, Quantitative XRD and devitrification allow better understanding of individual fly ash samples in terms of the available material to undergo geopolymerisation. When the type of glass phases present in fly ash are known and estimates of their relative concentrations are calculated, the setting time and compressive strength profiles of geopolymers synthesised can be predicted. These leads to the potential of generating an ideal ash, by blending specific fly ashes, in order to achieve a desired glass phase chemistry that will result in optimised geopolymer products.

Acknowledgments

The financial support of the Particulate Fluids Processing Centre (a Special Research Centre of the Australian Research Council) is gratefully acknowledged.

REFERENCES

[1] Bouzoubaa, N, Fournier, B., Malhotra, V., Golden, D.M. ACI Mat. J., 2002, *99,* 560-567.
[2] Van Jaarsveld, J.G.S., and Van Deventer, J.S.J., *Min. Eng*., 1992*, 10* , 659
[3] Palomo, A., Grutzeck, M.W., Blanco, M.T. *Cem. Concr. Res*., 1999, *29,* 1323
[4] Davidovits, J. Geopolymers: Inorganic Polymeric New Materials. *J. Therm. Anal.* 1991, 37, 1633
[5] Helmuth, R. Fly Ash in Cement and Concrete. 1987, Portland Cement Association, Skokie, IL
[6] Doremus, R.H., *Glass Science*, 1973, John Wiley & Sons
[7] Shelby, J.E. *Introduction to Glass Science and Technology*. RCA Paperbacks, 1997
[8] Patil, M.D; Eaton, H.C.; Tittlebaum, M.E. ^{57}Mössbauer spectroscopic studies of fly ash from coal-fired power plants and bottom ash from lignite-natural gas combustion. *Fuel* 1984, *63*(6), 788
[9] Hinckley, C.C.; Smith, G.V.; Twardowska, H.; Saporoschenko, M.; Shiley, R.H.; Griffen, R.A. Mössbauer studies of iron in Lurgi gasification ashes and power plant fly and bottom ash. *Fuel*, 1980, *59*
[10] Spiro, C.L.; Wong, J.; Lytle, F.W.; Greegor, R.B.; Maylotte, D.H.; Lamson, S.H. Forms of potassium in coal and its combustion products. *Fuel*, 1986, *65*, 327

[11] Diamond, S. On the Glass Present in Low-Calcium and in High-Calcium Flyashes, *Cem. Concr. Res.*, 1982, *13*, 459
[12] Qian, J.C.; Lachowski, E.E.; Glasser, F.P. Microstructural and chemical variation in Class F fly ash, *Fly Ash and Coal Conversion By-Products: Characterization, Utilization, and Disposal V: Symposium*, 1988, 45-53
[13] Hemmings, R.T.; Berry E.E., On the Glass in Coal Fly Ashes: Recent Advances, *Fly Ash and Coal Conversion By-Products: Characterization, Utilization, and Disposal V: Symposium*, 1987, 3-38
[14] Diamond, S. Particle Morphologies in Fly Ash, 1986, *16*, 569.

FIGURES

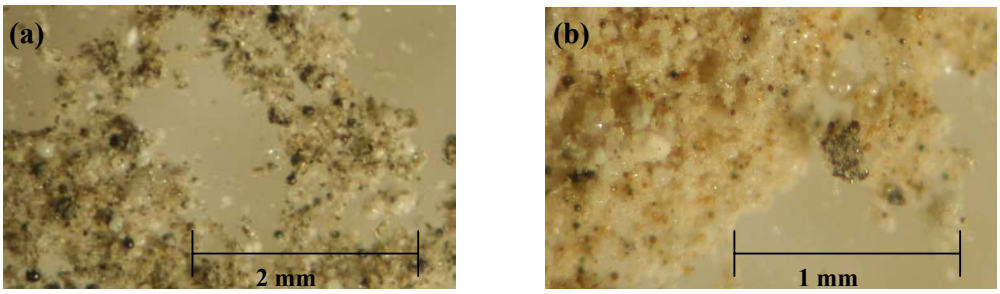

Figure 1. Optical Microscope Images: (a) Fly Ash A (Class F); (b) Fly Ash B (Class C)

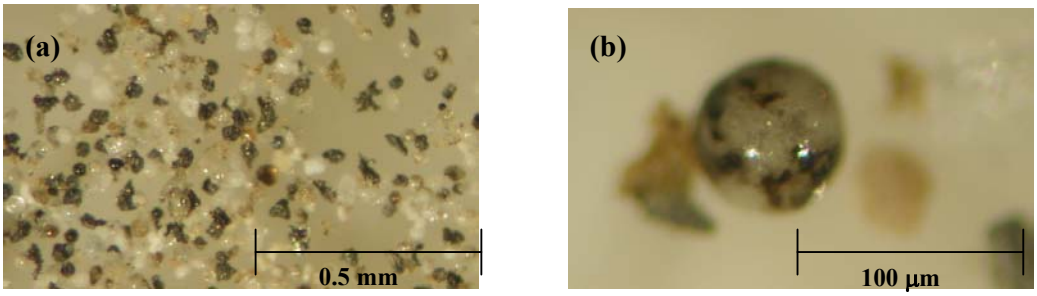

Figure 2. Optical Microscope Images: (a) Fly Ash A, particle size fraction -58µm +38µm; (b) Fly Ash B, particle showing glass phase intraparticle heterogeneity.

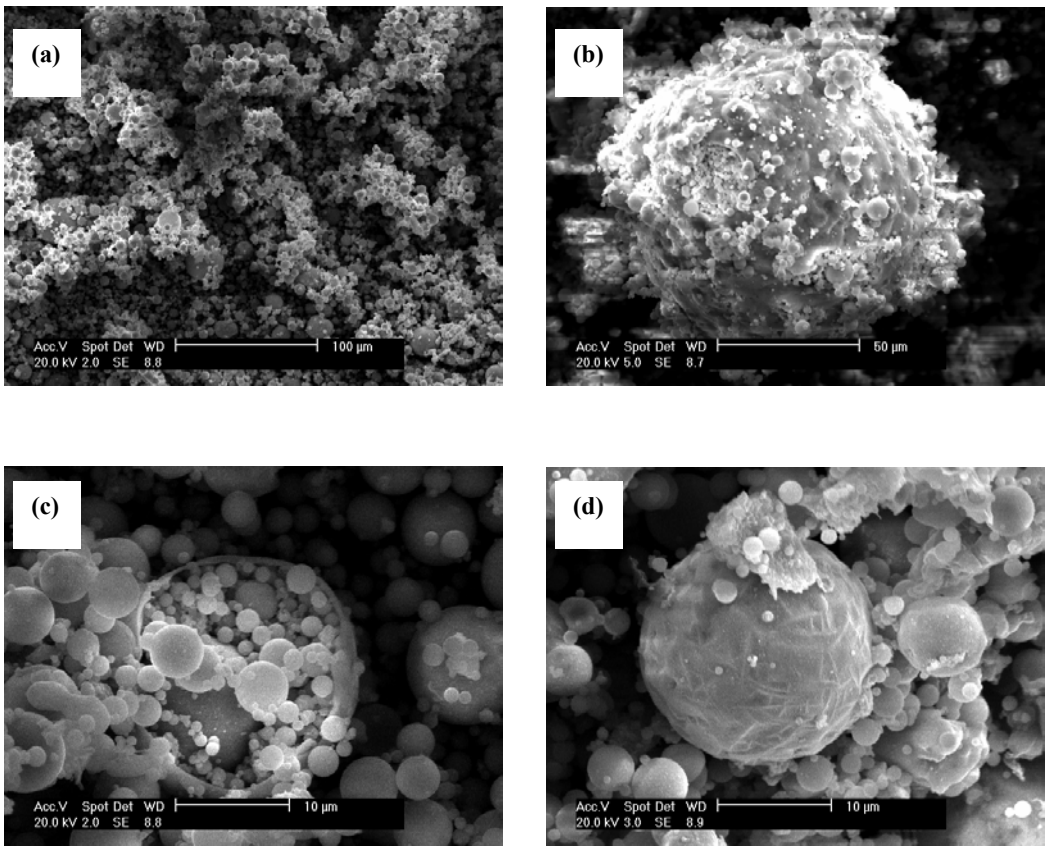

Figure 3. (a) Fly Ash A particle morphology demonstrating mainly spherical shape of particles; (b) Large plerosphere in Fly Ash A; (c) Small plerosphere in Fly Ash A; (d) Fly Ash A particle with visible crystals.

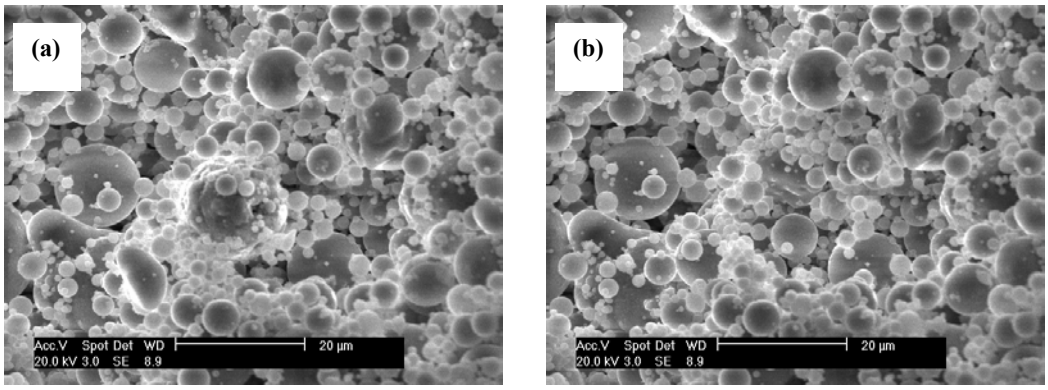

Figure 4. (a) Fly Ash B particle with irregular surface characteristic of a magnetite particle; (b) the same image as (a) after the electron beam has been moved closer to particle. The magnetite particle is repelled and shifts to the farthest position from the beam.

TABLES

Table 1. Physical properties of fly ashes studied.

ASH	PARTICLES < 38μm	COLOUR	PARTICLE SHAPE
Fly ash A	81%	Grey	Mainly spherical with some larger irregular shaped particles and some clusters of spheres
Fly ash B	64%	Brown	Mainly spherical with some larger irregular shaped particles and some clusters of spheres

Table 2. Transformations of coal minerals during the combustion of coal[7].

MINERAL	COMMENTS	CRYSTAL PRODUCTS	GLASSY PRODUCTS
Kaolinite	Melts in flame	Phase separation can occur producing mullite	Phase separation can occur resulting in a vitreous silica and mullite crystals, or an alumino-silicate vitreous glass can form.
Quartz	Does not melt in flame	Quartz	None
Calcite	Melts in flame	Lime and calcite	Calcium silicate type glass
Pyrite	Melts in flame	Magnetite and Hematite	Iron silicate glasses

Table 3. Oxide compositions of Fly Ash A and Fly Ash B as determined by XRF (wt %).

Ash	Na_2O	MgO	Al_2O_3	SiO_2	P_2O_5	SO_3	K_2O	CaO	TiO_2	MnO	Fe_2O_3
A	0.28	1.35	27.84	45.56	0.53	0.21	0.47	5.61	1.36	0.19	11.21
B	1.05	2.06	18.10	47.49	0.45	1.01	0.40	19.11	0.91	0.03	6.32

Table 4. Phase concentrations of Fly Ash A and Fly Ash B (wt %), as determined by Q-XRD (±5%).

Fly Ash	Amorphous	Quartz	Mullite	Magnetite	Calcite
A	67%	4%	15%	11%	3%
B	83%	9%	9%	<1%	<1%

Table 5. Phases formed from the devitrification of fly ash A and B and relative quantities.

Devitrified fly ash	Crystalline Phase(s)	Percentage for fly ash <38μm	Amorphous Phase	Percentage for fly ash <38μm
A	Mullite ($Al_6Si_2O_{13}$) Quartz (SiO_2) Magnetite (Fe_3O_4) Hematite (Fe_2O_3) Cristobalite (SiO_2) Diopside ($Ca(Mg,Al)(Si,Al)_2O_6$)	53% 8% - 28% 1% 10%	Vitrified silica – with various cations present including Na, K and Ca	54%
B	Quartz (SiO_2) Mullite ($Al_6Si_2O_{13}$) Hematite (Fe_2O_3) Magnetite (Fe_3O_4) Anorthite ($(Ca,Na)(Si,Al)_4O_8$) Gehlenite ($Ca_2Al_2SiO_7$) Diopside ($Ca(Mg,Al)(Si,Al)_2O_6$) Cristobalite (SiO_2) Wollastonite ($CaSiO_3$)	16% 10% - 3% 21% 21% 15% 1% 13% - -	Vitrified silica – with various cations present including Na, K and Ca	52%

Table 6. Compressive strengths (MPa) of mortars generated using Fly ash A and B. Silicate/Binder ratio kept constant.

[Hydroxide] (molar)	1 Day Strength Fly Ash A (MPa)	7 Day Strength Fly Ash A (MPa)	3 Day Strength Fly Ash B (MPa)
3	2.1	8.6	5.0
5	4.1	16.1	12.1
7	4.7	21.4	16.1